

LETTERS

Association of reactive oxygen species levels and radioresistance in cancer stem cells

Maximilian Diehn^{1,2*}, Robert W. Cho^{2,3*}, Neethan A. Lobo², Tomer Kalisky⁸, Mary Jo Dorie¹, Angela N. Kulp², Dalong Qian², Jessica S. Lam², Laurie E. Ailles², Manzhi Wong², Benzion Joshua⁴, Michael J. Kaplan⁴, Irene Wapnir⁵, Frederick M. Dirbas⁵, George Somlo⁹, Carlos Garberoglio¹⁰, Benjamin Paz¹⁰, Jeannie Shen¹⁰, Sean K. Lau¹¹, Stephen R. Quake⁸, J. Martin Brown¹, Irving L. Weissman^{2,6} & Michael F. Clarke^{2,7}

The metabolism of oxygen, although central to life, produces reactive oxygen species (ROS) that have been implicated in processes as diverse as cancer, cardiovascular disease and ageing. It has recently been shown that central nervous system stem cells^{1,2} and haematopoietic stem cells and early progenitors^{3–6} contain lower levels of ROS than their more mature progeny, and that these differences are critical for maintaining stem cell function. We proposed that epithelial tissue stem cells and their cancer stem cell (CSC) counterparts may also share this property. Here we show that normal mammary epithelial stem cells contain lower concentrations of ROS than their more mature progeny cells. Notably, subsets of CSCs in some human and murine breast tumours contain lower ROS levels than corresponding non-tumorigenic cells (NTCs). Consistent with ROS being critical mediators of ionizing-radiation-induced cell killing^{7,8}, CSCs in these tumours develop less DNA damage and are preferentially spared after irradiation compared to NTCs. Lower ROS levels in CSCs are associated with increased expression of free radical scavenging systems. Pharmacological depletion of ROS scavengers in CSCs markedly decreases their clonogenicity and results in radiosensitization. These results indicate that, similar to normal tissue stem cells, subsets of CSCs in some tumours contain lower ROS levels and enhanced ROS defences compared to their non-tumorigenic progeny, which may contribute to tumour radioresistance.

We began by addressing whether the low ROS concentrations that seem to be critical for self-renewal of haematopoietic stem cells (HSCs)^{3,5} are also a property of mammary epithelial stem cells^{9,10}. We isolated CD24^{med}CD49^{high}Lin[−] mammary cells—a population enriched for mammary repopulating units (MRUs)—and CD24^{high}CD49^{low}Lin[−] progenitor cells by flow cytometry (Supplementary Fig. 1), and then measured the intracellular concentrations of prooxidants using 2′-7′-dichlorofluorescein diacetate (DCF-DA) staining³. Cells in the MRU-enriched population contained significantly lower concentrations of ROS than the progenitor-enriched cells in two different strains of mice (Fig. 1a–c). Specifically, the MRU-enriched populations showed low to intermediate ROS levels, whereas the progenitor-enriched populations contained more uniformly high levels. Similarly, analysis of the two populations using MitoSOX Red—a highly selective detection method for mitochondrial superoxide—demonstrated lower superoxide levels in the MRU-enriched population (Fig. 1d). To assess whether mammary repopulating activity was related to intracellular concentrations of ROS, we transplanted CD24^{med}CD49^{high}Lin[−] cells on the basis of their

DCF-DA staining levels. Mammary stem cells with low and intermediate ROS levels gave rise to epithelial outgrowths when transplanted into cleared fat pads (Supplementary Table 1). Similar heterogeneity of ROS concentrations was recently demonstrated in HSC-enriched populations^{5,11}, where it may have functional importance in modulating the HSC-niche interaction¹².

Given the conservation of low ROS levels in several types of normal tissue stem cells, we proposed that CSCs in some tumours may also contain lower concentrations of ROS than their non-tumorigenic progeny. To investigate ROS biology in human CSCs, we began by examining the expression of genes involved in ROS metabolism in primary human breast CSCs and NTCs. Using microarray data from human breast CSC-enriched populations and NTCs¹³, and a curated list of genes involved in ROS metabolism⁵ (see Methods), gene set enrichment analysis (GSEA)¹⁴ revealed that the expression of ROS genes was highly over-represented in the CD44⁺CD24^{−/low}Lin[−] breast CSC-enriched population compared to the NTCs ($P < 0.001$; Supplementary Fig. 2). The ROS genes identified as the core-enriched genes by GSEA included several important antioxidant genes (Supplementary Table 2). Thus, gene expression profiles of human breast CSC-containing populations suggest that they contain higher levels of antioxidant defence systems than NTCs.

Next we directly assessed ROS levels in human tumour subpopulations. To do this the CD44⁺CD24^{−/low}Lin[−] breast CSC-enriched population and the corresponding ‘not CD44⁺CD24^{−/low}Lin[−]’ NTC population were purified from surgically resected breast tumours (Supplementary Fig. 3). DCF-DA staining showed that the CSC-enriched population in the human breast tumours we examined contained considerably lower levels of prooxidants than the NTC population. In some breast tumours, most of the cells in the CSC-containing fraction displayed a low ROS phenotype compared to the NTCs (Fig. 1e), whereas in others it was restricted to a significant subset of CSCs (Supplementary Fig. 4). We found a similar enrichment of cells with low ROS concentrations in a head and neck tumour (Supplementary Fig. 4). Thus, CSC-enriched populations from some human tumours contain lower average intracellular ROS levels than corresponding NTC populations.

Recently, we have demonstrated that Thy1⁺CD24⁺Lin[−] cells in most spontaneously developing breast tumours from mouse mammary tumour virus (MMTV)-Wnt1 mice are highly enriched for tumorigenic activity¹⁵ (Supplementary Fig. 5a). We therefore addressed whether the CSC-enriched population in this model system also shows a low ROS phenotype. ROS analysis using DCF-DA demonstrated that in tumours

¹Department of Radiation Oncology, ²Stanford Institute for Stem Cell Biology and Regenerative Medicine, ³Department of Pediatrics Division of Stem Cell Transplantation, ⁴Department of Otolaryngology—Head and Neck Surgery, ⁵Department of Surgery, ⁶Departments of Pathology and Developmental Biology, ⁷Department of Medicine, Stanford University School of Medicine, Stanford, California 94305, USA. ⁸Department of Bioengineering and Howard Hughes Medical Institute, Stanford University, Stanford, California 94305, USA. ⁹Department of Medical Oncology and Therapeutics Research, ¹⁰Department of Surgery, ¹¹Department of Pathology, City of Hope National Medical Center, Duarte, California, California 91010, USA.

*These authors contributed equally to this work.

in which the $\text{Thy1}^+ \text{CD24}^+ \text{Lin}^-$ population was enriched for CSCs, this population contained a significantly higher fraction of cells with low prooxidant levels than the 'not $\text{Thy1}^+ \text{CD24}^+$, Lin^- non-tumorigenic population (Fig. 1f). $\text{Thy1}^+ \text{CD24}^+ \text{Lin}^-$ cells contained two main subpopulations of cells on the basis of ROS concentration, with the low ROS subpopulation being significantly over-represented compared to NTCs (Supplementary Fig. 5b). To confirm the presence of CSCs within the low ROS subpopulation, we transplanted CSCs on the basis of their DCF-DA staining and found that both the low and the high ROS subsets of $\text{Thy1}^+ \text{CD24}^+ \text{Lin}^-$ cells gave rise to tumours in recipient animals (Supplementary Table 3). Thus, a subset of CSCs from these MMTV-Wnt1 tumours had lower baseline levels of ROS compared to NTCs.

It is well established that cell killing after exposure to ionizing radiation and a subset of cytotoxic chemotherapeutics is partially mediated by free radicals¹⁶. Given our observations of increased

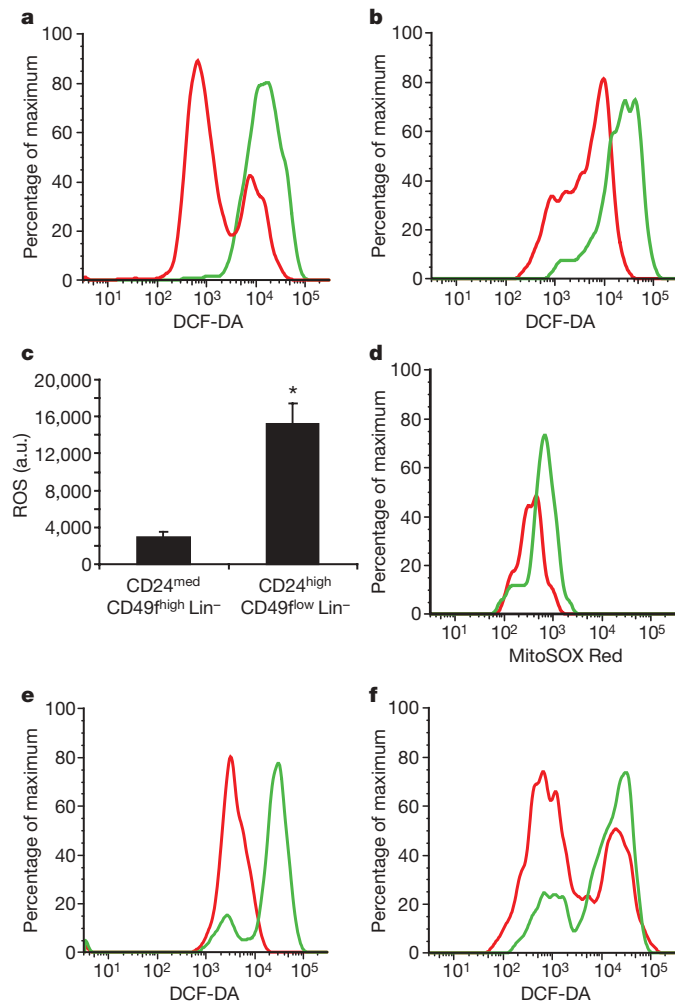


Figure 1 | Analysis of ROS levels in normal mammary and breast cancer stem cells and their progeny. **a**, $\text{CD24}^{\text{med}} \text{CD49}^{\text{high}} \text{Lin}^-$ mammary cells (mammary stem-cell-containing population; red) and $\text{CD24}^{\text{high}} \text{CD49}^{\text{low}} \text{Lin}^-$ mammary cells (progenitor cell-containing population; green) were isolated from C57BL/6J female mice using flow cytometry, and intracellular ROS concentrations were measured by DCF-DA staining. **b**, As in **a** except using 29S1/SvImJ mice. **c**, The mean and s.e.m. for replicates of **a** and **b** are shown ($n = 6$, $*P = 0.001$). a.u., arbitrary units. **d**, As in **b** but using MitoSOX Red instead of DCF-DA. Data shown are representative of two independent experiments. **e**, $\text{CD44}^+ \text{CD24}^{-/\text{low}} \text{Lin}^-$ breast cancer cells (CSC-containing population; red) and 'not $\text{CD44}^+ \text{CD24}^{-/\text{low}}, \text{Lin}^-$ cells (non-tumorigenic population; green) were isolated from a primary human breast tumour by flow cytometry and ROS levels were analysed using DCF-DA. **f**, As in **e** but using murine $\text{Thy1}^+ \text{CD24}^+ \text{Lin}^-$ breast cancer cells (CSC-containing population; red) and 'not $\text{Thy1}^+ \text{CD24}^+, \text{Lin}^-$ cells (non-tumorigenic population; green) isolated from an MMTV-Wnt1 breast tumour.

expression of ROS defence genes in CSCs, we were interested in testing whether CSC-enriched populations develop less DNA damage than NTCs after ionizing radiation. To examine DNA damage immediately after irradiation, we purified $\text{Thy1}^+ \text{CD24}^+ \text{Lin}^-$ cells and NTCs from MMTV-Wnt1 tumours by flow cytometry and irradiated them on ice. Cells were then either left on ice or incubated at 37 °C, before being analysed using the alkaline comet assay¹⁷. Although untreated cells did not show significantly different levels of DNA damage, there were fewer DNA strand breaks in the $\text{Thy1}^+ \text{CD24}^+ \text{Lin}^-$ cells than in the NTCs immediately after exposure to ionizing radiation (Fig. 2a, b). These findings are consistent with the hypothesis that the enhanced expression of ROS defences in CSCs contributes to reduced levels of DNA damage after irradiation.

Because the alkaline comet assay mainly measures single-strand breaks, and as double-strand breaks are important for ionizing-radiation-induced lethality¹⁸, we also analysed the levels of double-strand breaks as reflected by phosphorylated histone 2AX (H2AX, also known as H2AFX) nuclear foci after *in vitro* irradiation. As with the comet assay, we again observed significantly lower levels of DNA damage in $\text{Thy1}^+ \text{CD24}^+ \text{Lin}^-$ CSC-enriched cells than in NTCs (Supplementary Fig. 6). We also measured phosphorylated H2AX foci after *in vivo* irradiation of MMTV-Wnt1 tumours, and again found that $\text{Thy1}^+ \text{CD24}^+ \text{Lin}^-$ cells contained fewer foci than NTCs (Fig. 2c). Thus, consistent with their lower baseline levels of ROS, $\text{Thy1}^+ \text{CD24}^+ \text{Lin}^-$ CSC-enriched cells isolated from these tumours developed less DNA strand breaks than NTCs after exposure to ionizing radiation.

Given these findings, CSCs would be expected to preferentially survive exposure to ionizing radiation in intact tumours. Mice bearing MMTV-Wnt1 tumours were therefore treated with short, fractionated courses of ionizing radiation and the percentage of the $\text{Thy1}^+ \text{CD24}^+ \text{Lin}^-$ CSC-enriched population before and after irradiation was analysed using flow cytometry. On average, we found an

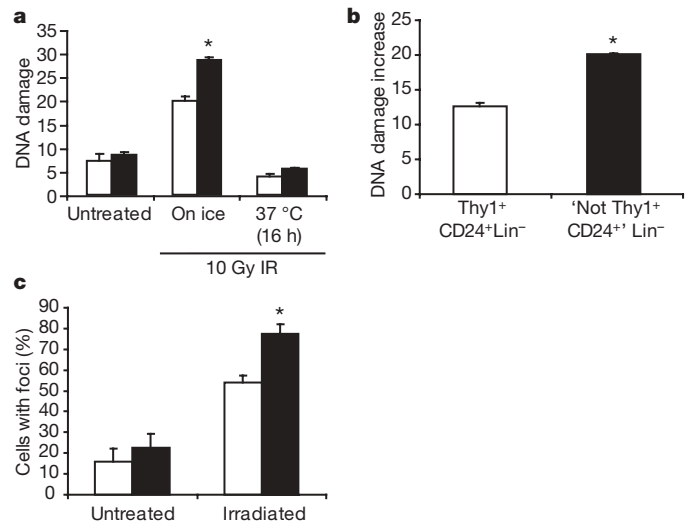


Figure 2 | $\text{Thy1}^+ \text{CD24}^+ \text{Lin}^-$ CSC-enriched cells develop less DNA damage after irradiation than non-tumorigenic cells. **a**, $\text{Thy1}^+ \text{CD24}^+ \text{Lin}^-$ cells (CSC-enriched population; open bars) and 'not $\text{Thy1}^+ \text{CD24}^+, \text{Lin}^-$ non-tumorigenic cells (filled bars) were isolated from MMTV-Wnt1 breast tumours by flow cytometry and irradiated with 10 Gy of ionizing radiation (IR). DNA damage was measured before irradiation, immediately after irradiation, and 16 h later using the alkaline comet assay. Data are the mean of median tail moments and s.e.m. ($n = 3$, $*P = 0.05$). **b**, Using the data from **a**, the difference in median tail moments between the untreated and 'on ice' time points was calculated. Data are mean and s.e.m. ($n = 3$, $*P = 0.004$). **c**, $\text{Thy1}^+ \text{CD24}^+ \text{Lin}^-$ cells (open bars) and 'not $\text{Thy1}^+ \text{CD24}^+, \text{Lin}^-$ non-tumorigenic cells (filled bars) from MMTV-Wnt1 tumours that were processed and collected 15 min after being irradiated *in vivo* with 1 Gy of ionizing radiation were immunostained for $\gamma\text{-H2AX}$, a marker of DNA double-strand breaks. Data are mean and s.e.m. ($n = 2$, $*P = 0.04$).

approximately twofold increase in the percentage of the $\text{Thy1}^+ \text{CD24}^+ \text{Lin}^-$ CSC-enriched population compared with the 'not $\text{Thy1}^+ \text{CD24}^+$ Lin^- NTCs in the irradiated tumours, suggesting that CSCs are relatively radioresistant compared with NTCs (Fig. 3a, b). We found a similar increase in the fraction of the $\text{CD44}^+ \text{Lin}^-$ CSC-enriched population when we irradiated human head and neck cancer xenografts grown in immunodeficient mice (Fig. 3c). Other investigators have documented similar radioresistance of CSCs in brain tumours¹⁹ and a breast cancer cell line²⁰. Thus, CSCs in some murine and human tumours are relatively radioresistant compared to their NTC counterparts.

Because a significant fraction of murine breast CSCs contained relatively low levels of ROS, we proposed that these cells may express enhanced levels of ROS defences compared to their NTC counterparts. We were particularly interested in glutathione (GSH), a critical cellular reducing agent and antioxidant that has been implicated in chemotherapy and radiotherapy resistance of cancer cells²¹. As our previous analyses demonstrated heterogeneity in CSC-enriched populations, and because single-cell gene expression studies have shown significant variations in gene expression in other stem cell populations²², we investigated the expression of critical GSH biosynthesis genes in MMTV-Wnt1 CSCs and NTCs using single-cell quantitative PCR with reverse transcription (qRT-PCR). This analysis showed significant overexpression of *Gclm* ($P < 0.001$) and *Gss* ($P < 0.005$) in a large fraction of cells within the CSC-enriched population, the former of which encodes the regulatory subunit of the enzyme (glutamate-cysteine ligase) that catalyses the rate-limiting step of GSH synthesis (Fig. 4a)²³. Furthermore *Foxo1*, a transcription factor implicated in the regulation of an anti-ROS gene expression program in HSCs⁵, was also overexpressed in CSCs compared to NTCs ($P < 0.001$; Fig. 4a). Other genes, including *Hif1a*, *Epas1* and *Foxo4*, were not differentially expressed. Thus, genes controlling GSH biosynthesis were overexpressed by many cells within the CSC-enriched population isolated from this tumour.

To pharmacologically manipulate ROS levels separately in CSCs and NTCs, we used *in vitro* culture conditions that allowed both cell

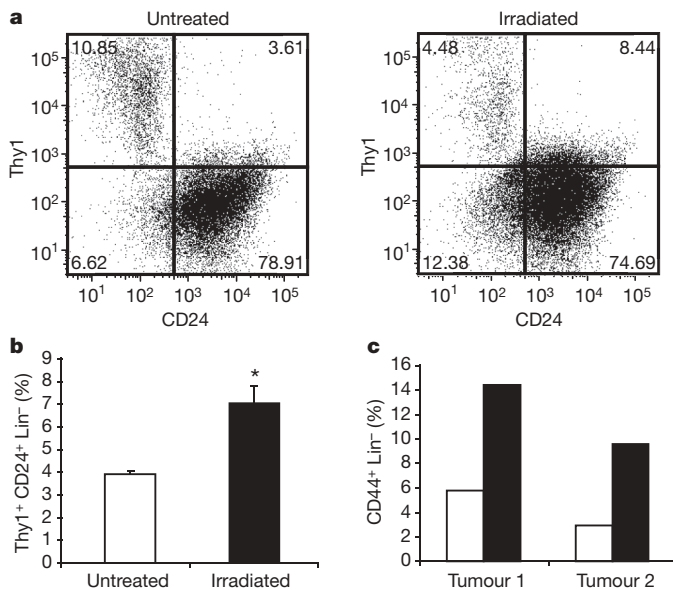


Figure 3 | Enrichment of CSCs after *in vivo* irradiation. **a**, Breast tumours from MMTV-Wnt1 mice were irradiated *in vivo* with 3×5 Gy or 5×2 Gy. The percentage of $\text{Thy1}^+ \text{CD24}^+ \text{Lin}^-$ cells in untreated and irradiated tumours was quantified by flow cytometry 72 h after the last fraction was delivered. **b**, The mean and s.e.m. for replicates of **a** are shown ($n = 6$, $*P = 0.008$). **c**, First generation xenografts established from two different primary human head and neck cancers were irradiated *in vivo* with 2×3 Gy (filled bars) or with untreated control (open bars). The percentage of $\text{CD44}^+ \text{Lin}^-$ cells was quantified as above.

populations to produce colonies after co-culture with irradiated feeder cells. We found that $\text{Thy1}^+ \text{CD24}^+ \text{Lin}^-$ CSC-enriched cells were relatively radioresistant compared with NTCs (Fig. 4b and Supplementary Fig. 7). When exposed to 2 Gy—a dose commonly administered clinically during daily treatments of breast cancer patients—twofold ± 0.2 more CSC-enriched colonies survived than NTC colonies. Next, we attempted to radioprotect NTCs by exposing them to the nitroxide antioxidant tempol²⁴. Pretreatment with tempol radioprotected NTCs, and resulted in survival levels similar to those seen in the CSC-enriched population (Fig. 4c).

Given the overexpression of genes involved in GSH synthesis by CSCs, we wished to assess the sensitivity of these cells to ROS increase by pharmacological depletion of GSH. Exposure of $\text{Thy1}^+ \text{CD24}^+ \text{Lin}^-$ CSC-enriched cells to L-S,R-buthionine sulphoximine (BSO), which inhibits glutamate-cysteine ligase²⁵, decreased their colony forming ability by approximately threefold (Fig. 4d). Finally, we addressed whether GSH depletion would radiosensitize CSCs. As shown in Fig. 4e, BSO pretreatment of $\text{Thy1}^+ \text{CD24}^+ \text{Lin}^-$ CSC-enriched cells led to significant radiosensitization. These data demonstrate the importance of low ROS levels and antioxidant defences to CSC survival and radiosensitivity in these tumours.

Our data indicate that normal breast stem cells and a subset of CSCs in some tumours arising in both mice and humans contain lower levels of

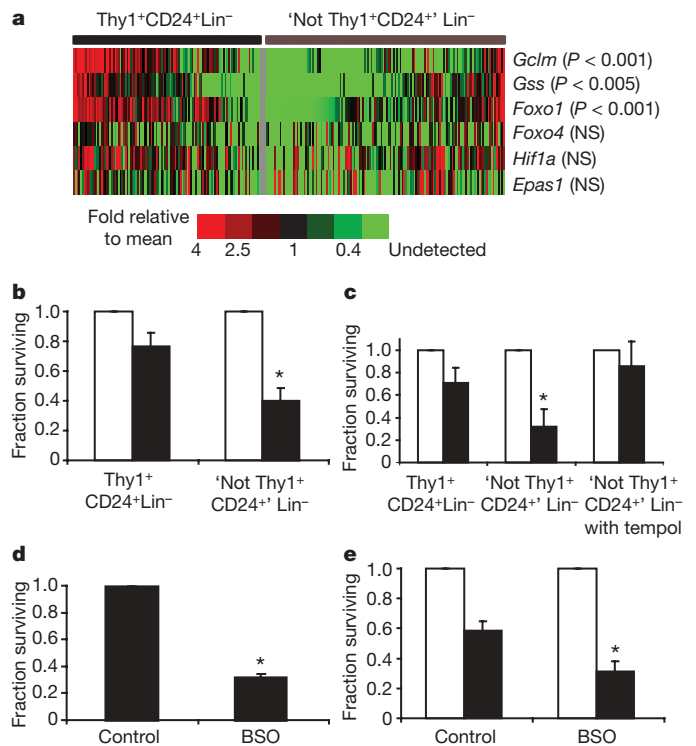


Figure 4 | $\text{Thy1}^+ \text{CD24}^+ \text{Lin}^-$ cells overexpress genes involved in ROS scavenging and pharmacological modulation of ROS levels affects the radiosensitivity of $\text{Thy1}^+ \text{CD24}^+ \text{Lin}^-$ and 'not $\text{Thy1}^+ \text{CD24}^+ \text{Lin}^-$ cells. **a**, Single-cell qRT-PCR analysis of gene expression in $\text{Thy1}^+ \text{CD24}^+ \text{Lin}^-$ CSC-enriched cells and 'not $\text{Thy1}^+ \text{CD24}^+ \text{Lin}^-$ non-tumorigenic cells. The heatmap displays the mean centred cycling threshold (C_t) values. **b**, Clonogenic survival of $\text{Thy1}^+ \text{CD24}^+ \text{Lin}^-$ CSC-enriched cells and 'not $\text{Thy1}^+ \text{CD24}^+ \text{Lin}^-$ non-tumorigenic cells before (open bars) and after (filled bars) 2 Gy of ionizing radiation, and in the presence of 10 mM of the ROS scavenger tempol ($n = 2$, $*P = 0.03$). **c**, Clonogenic survival of 'not $\text{Thy1}^+ \text{CD24}^+ \text{Lin}^-$ non-tumorigenic cells before (open bars) and after (filled bars) 2 Gy of ionizing radiation, and in the presence of 10 mM of the ROS scavenger tempol ($n = 2$, $*P = 0.03$). **d**, Clonogenic survival of $\text{Thy1}^+ \text{CD24}^+ \text{Lin}^-$ CSC-enriched cells in the presence or absence of 24-h pretreatment with 1 mM of the glutathione synthesis inhibitor BSO ($n = 3$, $*P = 0.002$). **e**, Clonogenic survival of $\text{Thy1}^+ \text{CD24}^+ \text{Lin}^-$ CSC-enriched cells before (open bars) or after (filled bars) 3 Gy of ionizing radiation, with or without BSO pretreatment ($n = 3$, $P = 0.03$). All data are mean and s.e.m.

ROS than their cellular descendants. Taken together with previous reports of low ROS concentrations in other normal tissue stem cells, these findings indicate that stem cells in diverse systems have conserved this attribute, which probably helps to protect their genomes from endogenous and exogenous ROS-mediated damage. The mechanism leading to low ROS levels in some CSCs seems to be at least partially due to the increased production of free radical scavengers. Notably, there seems to be marked heterogeneity of ROS levels in both normal stem cell and CSC-enriched populations, which could indicate that the enriched populations contain both stem and non-stem cells, and/or that ROS levels in stem cells can differ on the basis of environmental factors that alter the balance of endogenous production and the expression of scavenging pathways. The low ROS subset found in the various stem cell populations may also represent a quiescent subpopulation. Heterogeneity of ROS levels may influence the extent to which CSC-enriched populations are resistant to therapies such as ionizing radiation.

In light of recent findings that CSCs in glioblastoma multiforme display enhanced DNA repair capabilities¹⁹, it seems that CSCs may resist standard cytotoxic therapies through a combination of mechanisms, and that these may be unique to a given tumour. In the case of human CSCs, the frequency with which these cells show low ROS levels or enhanced DNA repair remains to be determined, particularly as the normal transformation precursor may be either stem or progenitor cells^{26,27} and because ROS concentration (Fig. 1 and refs 5, 28) and increased DNA repair capabilities seem to partially reflect differentiation state. Clinical therapies could probably be optimized by patient- and tumour-specific identification of CSC-resistance mechanisms, and overcoming low ROS levels in CSCs may be a useful method for improving local and systemic oncological therapies.

METHODS SUMMARY

Cells were analysed, collected by FACS and injected into recipient mice as described with minor modifications from mouse mammary glands¹⁰, human breast²⁹ cancers, human head and neck³⁰ cancers and MMTV-Wnt1 mouse tumours¹⁵. For human samples, informed consent was obtained after the approval of protocols by the Stanford University and City of Hope Institutional Review Boards. For intracellular ROS analysis, cells were loaded with 10 μ M DCF-DA (Invitrogen), incubated at 37 °C for 30 min, and immediately analysed by flow cytometry. Cells were resorted on the basis of their level of DCF-DA staining for transplant experiments. For MitoSOX Red experiments, cells were loaded with 5 μ M MitoSOX Red at 37 °C for 20 min. DNA damage was evaluated using the single-cell gel electrophoresis assay under alkaline conditions¹⁷. For γ -H2AX immunostaining, purified cells were cytospun onto poly-L-lysine coated slides, fixed, permeabilized and stained with a phospho-specific (Ser 139) histone H2AX antibody (Cell Signaling Technology) followed by a secondary Alexa Fluor 488-conjugated antibody (Invitrogen). For single-cell gene expression analysis, cells were sorted into 96-well plates containing CellsDirect qRT-PCR mix (Invitrogen). After reverse transcription, genes were pre-amplified (22 cycles) using the same Taqman primers (Applied Biosystems) used for quantification. Products were analysed using qPCR DynamicArray microfluidic chips (Fluidigm). For *in vitro* colony assays, cells were cultured in Epicult B medium (StemCell Technologies) with 5% serum in the presence of \sim 13,000 cm^{-2} irradiated NIH-3T3 cells. After 24–48 h, the media was replaced with serum-free Epicult B, and colonies were counted \sim 7 days later. GSEA¹⁴ was performed using previously published microarray data¹³ of CSCs and NTCs from primary breast tumour samples and a curated list of ROS genes (Supplementary Table 4). Levels of significance were determined by Student's *t*-tests using $\alpha = 0.05$.

Full Methods and any associated references are available in the online version of the paper at www.nature.com/nature.

Received 6 September 2007; accepted 18 December 2008.

Published online 4 February 2009; corrected 9 April 2009 (details online).

- Smith, J., Ladi, E., Mayer-Proschel, M. & Noble, M. Redox state is a central modulator of the balance between self-renewal and differentiation in a dividing glial precursor cell. *Proc. Natl Acad. Sci. USA* **97**, 10032–10037 (2000).
- Tsatmali, M., Walcott, E. C. & Crossin, K. L. Newborn neurons acquire high levels of reactive oxygen species and increased mitochondrial proteins upon differentiation from progenitors. *Brain Res.* **1040**, 137–150 (2005).
- Ito, K. *et al.* Regulation of oxidative stress by ATM is required for self-renewal of haematopoietic stem cells. *Nature* **431**, 997–1002 (2004).

- Ito, K. *et al.* Reactive oxygen species act through p38 MAPK to limit the lifespan of hematopoietic stem cells. *Nature Med.* **12**, 446–451 (2006).
- Tothova, Z. *et al.* FoxOs are critical mediators of hematopoietic stem cell resistance to physiologic oxidative stress. *Cell* **128**, 325–339 (2007).
- Miyamoto, K. *et al.* Foxo3a is essential for maintenance of the hematopoietic stem cell pool. *Cell Stem Cell* **1**, 101–112 (2007).
- Powell, S. & McMillan, T. J. DNA damage and repair following treatment with ionizing radiation. *Radiat. Oncol.* **19**, 95–108 (1990).
- Ward, J. F. Biochemistry of DNA lesions. *Radiat. Res.*, Suppl. 8, S103–S111 (1985).
- Shackleton, M. *et al.* Generation of a functional mammary gland from a single stem cell. *Nature* **439**, 84–88 (2006).
- Stingl, J. *et al.* Purification and unique properties of mammary epithelial stem cells. *Nature* **439**, 993–997 (2006).
- Jang, Y. Y. & Sharkis, S. J. A low level of reactive oxygen species selects for primitive hematopoietic stem cells that may reside in the low-oxygenic niche. *Blood* **110**, 3056–3063 (2007).
- Hosokawa, K. *et al.* Function of oxidative stress in the regulation of hematopoietic stem cell-niche interaction. *Biochem. Biophys. Res. Commun.* **363**, 578–583 (2007).
- Liu, R. *et al.* The prognostic role of a gene signature from tumorigenic breast-cancer cells. *N. Engl. J. Med.* **356**, 217–226 (2007).
- Subramanian, A. *et al.* Gene set enrichment analysis: a knowledge-based approach for interpreting genome-wide expression profiles. *Proc. Natl Acad. Sci. USA* **102**, 15545–15550 (2005).
- Cho, R. W. *et al.* Isolation and molecular characterization of cancer stem cells in MMTV-Wnt1 murine breast tumors. *Stem Cells* **26**, 364–371 (2008).
- Riley, P. A. Free radicals in biology: oxidative stress and the effects of ionizing radiation. *Int. J. Radiat. Biol.* **65**, 27–33 (1994).
- Dorie, M. J. *et al.* DNA damage measured by the comet assay in head and neck cancer patients treated with tirapazamine. *Neoplasia* **1**, 461–467 (1999).
- Cohen-Jonathan, E., Bernhard, E. J. & McKenna, W. G. How does radiation kill cells? *Curr. Opin. Chem. Biol.* **3**, 77–83 (1999).
- Bao, S. *et al.* Glioma stem cells promote radioresistance by preferential activation of the DNA damage response. *Nature* **444**, 756–760 (2006).
- Phillips, T. M., McBride, W. H. & Pajonk, F. The response of CD24^{low}/CD44⁺ breast cancer-initiating cells to radiation. *J. Natl. Cancer Inst.* **98**, 1777–1785 (2006).
- Estrela, J. M., Ortega, A. & Obrador, E. Glutathione in cancer biology and therapy. *Crit. Rev. Clin. Lab. Sci.* **43**, 143–181 (2006).
- Warren, L., Bryder, D., Weissman, I. L. & Quake, S. R. Transcription factor profiling in individual hematopoietic progenitors by digital RT-PCR. *Proc. Natl Acad. Sci. USA* **103**, 17807–17812 (2006).
- Griffith, O. W. Biologic and pharmacologic regulation of mammalian glutathione synthesis. *Free Radic. Biol. Med.* **27**, 922–935 (1999).
- Hahn, S. M. *et al.* Potential use of nitroxides in radiation oncology. *Cancer Res.* **54**, 2006s–2010s (1994).
- Bailey, H. H. L-S-R-buthionine sulfoximine: historical development and clinical issues. *Chem. Biol. Interact.* **111–112**, 239–254 (1998).
- Jamieson, C. H. *et al.* Granulocyte-macrophage progenitors as candidate leukemic stem cells in blast-crisis CML. *N. Engl. J. Med.* **351**, 657–667 (2004).
- Akala, O. O. *et al.* Long-term haematopoietic reconstitution by *Trp53*^{-/-}*p16Ink4a*^{-/-}*p19Arf*^{-/-} multipotent progenitors. *Nature* **453**, 228–232 (2008).
- Saretzki, G. *et al.* Downregulation of multiple stress defense mechanisms during differentiation of human embryonic stem cells. *Stem Cells* **26**, 455–464 (2008).
- Al-Hajj, M., Wicha, M. S., Benito-Hernandez, A., Morrison, S. J. & Clarke, M. F. Prospective identification of tumorigenic breast cancer cells. *Proc. Natl Acad. Sci. USA* **100**, 3983–3988 (2003).
- Prince, M. E. *et al.* Identification of a subpopulation of cells with cancer stem cell properties in head and neck squamous cell carcinoma. *Proc. Natl Acad. Sci. USA* **104**, 973–978 (2007).

Supplementary Information is linked to the online version of the paper at www.nature.com/nature.

Acknowledgements We thank D. Spitz for helpful discussions and D. Menke, D. Rossi, and J. Seita for technical assistance. This work was supported by grants from the National Institutes of Health (M.F.C., G.S. and I.L.W.), the Virginia and D.K. Ludwig Foundation (M.F.C. and I.L.W.), the Breast Cancer Research Foundation (M.F.C.), the Machiah foundation (T.K.), the American Society for Therapeutic Radiology and Oncology (M.D.), and the Radiological Society of North America (M.D.). M.D. is a recipient of the Leonard B. Holman Research Pathway fellowship.

Author Contributions M.D. and R.W.C. contributed equally to this work. M.D., R.W.C., N.A.L., T.K., M.J.D., A.N.K., D.Q., J.S.L., L.A. and M.W. performed the experiments. B.J., M.J.K., I.W., F.D., G.S., C.G., B.P., J.S. and S.K.L. aided in human tumour tissue acquisition. G.S. designed a pre-operative protocol allowing for tissue acquisition. M.D., R.W.C. and M.F.C. designed the experiments and wrote the manuscript. S.R.Q., J.M.B. and I.L.W. provided intellectual input and aided in experimental design.

Author Information Reprints and permissions information is available at npg.nature.com/reprintsandpermissions. The authors declare competing financial interests: details accompany the full-text HTML version of the paper at www.nature.com/nature. Correspondence and requests for materials should be addressed to M.F.C. (mfclarke@stanford.edu).

METHODS

Murine mammary stem cell isolation. Mammary glands from 6–12-week-old female C57BL/6j or 129S1/SvImJ mice were dissociated as described¹⁰ with minor modifications. Specifically, mammary fat pads were collected and placed directly into Medium 199 (Gibco BRL) supplemented with 20 mM HEPES and penicillin, streptomycin and actinomycin. Tissue was minced using sterile razor blades and 4 Wünsch units of Liberase Blendzyme 4 (Roche) and 100 Kunitz units of DNase I (Sigma) were added. Tissue was incubated for 60–90 min in a 37 °C and 5% CO₂ incubator, during which the cells were mechanically aspirated every 30 min. Cells were pelleted by centrifugation for 5 min at 4 °C and 350g. After lysis of the red blood cells with ACK lysis buffer (Gibco BRL), a single-cell suspension was obtained by further enzymatic digestion for ~2 min in 0.25% trypsin, followed by another ~2 min in 5 mg ml⁻¹ dispase II (StemCell Technologies) plus 200 Kunitz units DNase I (Sigma). Cells were then filtered through 40-µm nylon mesh, pelleted and resuspended in staining media (HBSS and 2% heat-inactivated calf serum (HICS)). Cells were counted using trypan blue dye exclusion.

Tumour dissociation. Human and mouse tumours were dissociated as previously described¹⁵ with minor modifications. Depending on the time of the surgical case, some of the human tumours were kept overnight at 4 °C before dissociation. Tumours from patients or from MMTV-Wnt1 tumour-bearing FVB/NJ female mice were minced with a razor blade and suspended in 20 ml of Medium 199 (Gibco BRL) supplemented with 20 mM HEPES. The dissociation enzyme cocktail consisted of 100 Kunitz units of DNase I (Sigma), 8 Wünsch units of Liberase Blendzyme 2 (Roche) and 8 Wünsch units Liberase Blendzyme 4 (Roche). Tumours were digested to completion (1.5–2.5 h at 37 °C and 5% CO₂) with pipetting every 30 min for manual dissociation. Once digested, 30 ml of RPMI (BioWhittaker) with 10% HICS was added to the digestion solution to inactivate the collagenases. A 40-µm nylon filter was used to filter the sample. After pelleting, cells were resuspended in 5 ml of ACK buffer for red blood cell lysis. HBSS (BioWhittaker) with 2% HICS was used to dilute the ACK buffer and the cells were again filtered through a 40-µm nylon filter. The filtered cells were spun down and resuspended in HBSS with 2% HICS.

Cell staining and flow cytometry. Cells were stained at a concentration of 1 × 10⁶ cells per 100 µl of HBSS with 2% HICS (staining media). Cells were blocked with rabbit or mouse IgG (1 mg ml⁻¹) at 1:100 dilution and antibodies were added at appropriate dilutions determined from titration experiments. For the normal mammary stem cell experiments, antibodies included CD49f, CD31, CD45, Ter119 (BD Pharmingen), CD24, Thy1.2 and CD140a (eBioscience). For the murine MMTV-Wnt1 breast cancer experiments, antibodies included CD24, Thy1.1, CD140a (eBioscience), CD45 and CD31 (BD Pharmingen). For the human breast cancer experiments, antibodies included CD44, CD24, CD45, CD3, CD20, CD10, glycoporin A (BD Pharmingen), CD31 (eBioscience) and CD64 (Dako). For the primary human head and neck cancer experiment, antibodies included CD44, CD45 (BD Pharmingen) and CD31 (eBioscience), and for the xenograft experiments, antibodies included CD44, mCD45 (BD Pharmingen), mCD31 (Abcam) and H-2K^d (eBioscience). Cells were stained for 20 min on ice and washed with staining media. When biotinylated primary antibodies were used, cells were further stained with streptavidin-conjugated fluorophores and washed. Ultimately, cells were resuspended in staining media containing 7-aminoactinomycin D (1 µg ml⁻¹ final concentration) or 4'-6-diamidino-2-phenylindole (DAPI, 1 µg ml⁻¹ final concentration) to stain dead cells.

For all experiments, cells were analysed and sorted using a FACSAria cell sorter (BD Bioscience). Side scatter and forward scatter profiles were used to eliminate debris and cell doublets. Dead cells were eliminated by excluding DAPI⁺ cells, whereas contaminating human or mouse Lin⁺ cells were eliminated by excluding cells labelled with the fluorophore used for the lineage antibody cocktail. In cell-sorting experiments, cell populations underwent two consecutive rounds of purification (double sorting) when the initial purity was not deemed high enough and a sufficient number of cells were available. Final purities ranged from ~60% to >95%.

MMTV-Wnt1 breast tumour radiation experiments. For *in vivo* irradiation experiments, tumour-bearing animals were irradiated on consecutive days with the indicated doses of ionizing radiation using a 160 kVp cabinet irradiator (Faxitron). Tumours were grown on the ventral surface of mice in the vicinity of the second mammary fat pad and the delivered dose was adjusted to compensate for attenuation by overlying tissues. Seventy-two hours after the final fraction was delivered, tumours were collected, dissociated and analysed by flow cytometry as above. For each experiment, at least one untreated control tumour was analysed in parallel. When multiple control tumours were available, the percentage of Thy1⁺ CD24⁺ Lin⁻ cells in these tumours was averaged to define the baseline percentage of Thy1⁺ CD24⁺ Lin⁻ cells for that experiment. In other experiments, tumours were irradiated and these tumours along with controls

were collected 15 min after irradiation. Tumours were dissociated as above and cells were stained with a phospho-specific (Ser 139) histone H2AX antibody (Cell Signaling Technology) as described in the Methods Summary.

Human breast and head and neck cancer primary specimens. Primary tumour specimens were obtained with informed consent after approval of protocols by the Stanford University and City of Hope Institutional Review Boards. Tumours were from untreated patients, except for the two breast cancer tumours shown in Supplementary Fig. 2a–d, which had been treated with neoadjuvant chemotherapy before resection.

Human head and neck cancer xenograft radiation experiments. Tumours were grown subcutaneously on the backs of Rag2/cytokine receptor common γ -chain double knockout (Rag2 γ DKO) mice as previously described³⁰. Mice were irradiated as described earlier, except that for each fraction half of the dose was delivered from the left side of the animal and half from the right. The non-tumour-bearing portions of each animal were shielded using custom-made lead chambers.

MMTV-Wnt1 DCF-DA transplant experiments. Lin⁻ or Thy1⁺ CD24⁺ Lin⁻ cells from tumours were sorted as described above. Cells were loaded with 10 µM DCF-DA (Invitrogen), incubated at 37 °C for 30 min, and sorted into 'ROS low' and 'ROS high' sub-populations on the basis of their DCF-DA staining profile. Sorted cells were injected into FVB female mice in Matrigel (BD Bioscience) in the vicinity of the second mammary fat pad at the indicated cell numbers.

Normal mammary stem cell DCF-DA transplant experiments. CD24^{med} CD49^{high} Lin⁻ mammary cells (enriched for mammary repopulating units) were isolated from mammary fat pads from C57BL/6j female mice as described above. Cells were loaded with 10 µM DCF-DA (Invitrogen), incubated at 37 °C for 30 min, and sorted into 'ROS low' and 'ROS mid' sub-populations on the basis of their DCF-DA staining profile (in comparison to that of CD24^{high} CD49^{low} Lin⁻ progenitor cells, which showed an 'ROS high' profile). Mammary glands of 21-day-old female C57BL/6j mice were cleared of endogenous epithelium as previously described¹⁰, and sorted cells were injected into each cleared fat pad using a Hamilton syringe. Injected glands were removed for wholemount analysis after 5–6 weeks. Transplants were scored as positive if epithelial structures consisting of ducts with lobules and/or terminal end buds and that arose from a central point were present.

In vitro colony assay. Sorted tumour cells were cultured in Epicult B medium (StemCell Technologies) with 5% serum in the presence of ~13,000 cm⁻² irradiated NIH-3T3 cells. After 24–48 h, the media was replaced with serum-free Epicult B, and ~7 days later, colonies were fixed with acetone:methanol (1:1), stained with Giemsa and counted. Colonies were counted if they contained \geq 30 cells and the number of colonies in control wells was in the range of 30–100, depending on how many cells were sorted and the plating efficiency of a given tumour. For the BSO experiments, cells were cultured for 24 h in modified mammosphere medium³¹ in the presence or absence of 1 mM BSO, and the drug was removed immediately before irradiation. For the tempol experiments, cells were treated with 10 mM tempol for 15 min before irradiation, after which the drug was removed. For all drug experiments, 'drug only' controls were run in parallel to adjust for effects of each drug on baseline colony counts.

Gene set enrichment analysis. To define a list of genes involved in ROS metabolism and regulation, we began with a previously generated list⁵. In brief, this list was initially generated by these authors using the Gene Ontology GO:TERMFINDER program (<http://search.cpan.org/dist/GO-TermFinder/>) to classify genes by biological process, molecular function, or cellular component. The biological process terms included were: response to oxidative stress; response to reactive oxygen species; response to hydrogen peroxide; response to oxygen radical; and response to superoxide. We manually curated this list by performing PubMed-based literature searches for each gene and only retaining those that had published evidence of involvement in ROS metabolism or regulation (that is, removing genes that seemed to be included solely owing to electronic curation with inferred evidence). This trimmed the ROS gene list from 55 to 36 unique symbols (Supplementary Table 4). GSEA was then applied as previously described¹⁴. The 'core enriched genes' shown in Fig. 4 were defined by the algorithm.

Single-cell gene expression analysis. For the single-cell gene expression experiments we used qPCR DynamicArray microfluidic chips (Fluidigm). Single MMTV-Wnt1 Thy1⁺ CD24⁺ Lin⁻ CSC-enriched cells and 'not Thy1⁺ CD24⁺ Lin⁻ non-tumorigenic cells were sorted by FACS into 96-well plates containing PCR mix (CellsDirect, Invitrogen) and RNase inhibitor (SuperaseIn, Invitrogen). After hypotonic lysis, we added qRT-PCR enzymes (SuperScript III RT/Platinum Taq, Invitrogen), and a mixture containing a pool of low-concentration assays (primers/probes) for the genes of interest (Gclm-Mm00514996_m1, Gss-Mm00515065_m1, Foxo1-Mm00490672_m1, Foxo4-Mm00840140_g1, Hif1a-Mm00468875_m1, Epas1-Mm00438717_m1). Reverse transcription (15 min at 50 °C, 2 min of 95 °C) was followed by pre-amplification for 22 PCR cycles (each

cycle: 15 s at 95 °C, 4 min at 60 °C). Total RNA controls were run in parallel. The resulting amplified cDNA from each one of the cells was inserted into the chip sample inlets with Taqman qPCR mix (Applied Biosystems). Individual assays (primers/probes) were inserted into the chip assay inlets (two replicates for each). The chip was loaded for 1 h in a chip loader (Nanoflex, Fluidigm) and then transferred to a reader (Biomark, Fluidigm) for thermocycling and fluorescent quantification.

To remove low quality gene assays, we discarded gene assays in which the qPCR curves showed non-exponential increases. To remove low quality cells (for example, dead cells) we discarded cells that did not express the housekeeping genes *Actb* (beta-actin) and *Hprt1* (hypoxanthine guanine phosphoribosyl transferase 1). This resulted in a single-cell gene expression data set consisting of 248 cells (109 tumorigenic and 139 non-tumorigenic) from a total of seven chip-runs. A two-sample Kolmogorov–Smirnov (K-S) statistic was calculated to test whether genes were differentially expressed in the two populations. We generated *P* values by permuting the sample labels (that is, Thy1⁺ CD24⁺ Lin⁻ CSC-enriched cells versus ‘not Thy1⁺ CD24⁺ Lin⁻ non-tumorigenic cells) and comparing the actual K-S statistic to those in the permutation-derived null distribution. The *P* values were further corrected by Bonferroni correction to adjust for multiple hypothesis testing.

31. Liao, M. J. *et al.* Enrichment of a population of mammary gland cells that form mammospheres and have in vivo repopulating activity. *Cancer Res.* **67**, 8131–8138 (2007).